UC Berkeley
UC Berkeley Previously Published Works

Title

Bidirectional homeostatic plasticity induced by interneuron cell death and transplantation in vivo

Permalink

Journal

ISSN

Authors

Howard, MacKenzie Allen
Rubenstein, John LR
Baraban, Scott C

Publication Date

DOI

Peer reviewed

Bidirectional homeostatic plasticity induced by interneuron cell death and transplantation in vivo

MacKenzie Allen Howard[a], John L. R. Rubenstein[b], and Scott C. Baraban[a,1]

[a]Epilepsy Research Laboratory, Department of Neurological Surgery and [b]Nina Ireland Laboratory of Developmental Neurobiology, Department of Psychiatry, University of California, San Francisco, CA 94143

Chronic changes in excitability and activity can induce homeostatic plasticity. These perturbations may be associated with neurological disorders, particularly those involving loss or dysfunction of GABA interneurons. In distal-less homeobox 1 ($Dlx1^{-/-}$) mice with late-onset interneuron loss and reduced inhibition, we observed both excitatory synaptic silencing and decreased intrinsic neuronal excitability. These homeostatic changes do not fully restore normal circuit function, because synaptic silencing results in enhanced potential for long-term potentiation and abnormal gamma oscillations. Transplanting medial ganglionic eminence interneuron progenitors to introduce new GABAergic interneurons, we demonstrate restoration of hippocampal function. Specifically, miniature excitatory postsynaptic currents, input resistance, hippocampal long-term potentiation, and gamma oscillations are all normalized. Thus, in vivo homeostatic plasticity is a highly dynamic and bidirectional process that responds to changes in inhibition.

excitatory/inhibitory balance | gamma frequency oscillations | LTP | neural transplantation

Prolonged changes in activity levels induce bidirectional changes in neuronal excitability and synaptic activity known as homeostatic plasticity (1, 2). This phenomenon has been described well at excitatory synapses and functions to maintain activity within a preferred dynamic range. Maintaining excitatory/inhibitory synaptic balance is critical for neuronal information processing and a potential problem when confronted with aberrant states of excitability, such as those associated with autism, schizophrenia, Alzheimer's disease, or epilepsy (3–12).

Chronic manipulation of synaptic input and/or action potential (AP) output rates in cortical and hippocampal cell cultures induces homeostatic synaptic scaling, in which the amplitude and then the frequency of pyramidal neuron miniature excitatory postsynaptic currents (mEPSCs) increase when activity is lowered or decrease when activity is raised (13–16). Recent studies have begun to reveal the underlying molecular mechanisms of homeostatic synaptic changes, including the AMPA receptor subunits, synapse-associated calcium-binding proteins, and intracellular signaling cascades involved (14, 17, 18). Changes to activity also trigger homeostatic plasticity of inhibitory synaptic transmission (19–23). Homozygous deletion of glutamate decarboxylase 1 (*Gad1*), the rate-limiting enzyme in the synthesis of GABA, reduced miniature inhibitory postsynaptic current (mIPSC) amplitudes in cultured hippocampal neurons but also blocked further homeostatic changes to mIPSCs. This suggests a key role for regulation of *Gad1* expression in inhibitory homeostatic plasticity (23). Intrinsic excitability is also homeostatically regulated by activity. Changes in input resistance (Rin) and voltage-activated K^+ and Na^+ channel number (24–27), and in Na^+ channel compartmentalization (28, 29), have been described following manipulations that chronically alter neuronal activity. Finally, in vivo manipulation of neuronal activity with TTX results in larger mEPSC amplitudes and reduced Rin of CA1 pyramidal neurons (30), suggesting that multiple mechanisms of homeostatic plasticity can occur simultaneously in the intact nervous system.

Loss of GABAergic interneurons is common across different neurological disorders. It is unknown whether homeostatic plasticity can be induced by changes in activity related to interneuronopathy or how the combination of interneuron cell death and compensation alters circuit function. To begin to address these issues, we studied synaptic and intrinsic excitability in a hippocampal circuit in which a subpopulation of interneurons is reduced [i.e., distal-less homeobox 1 ($Dlx1^{-/-}$) mice] (31–33). At around 30 d of age, these mice lose a subset of somatostatin (Sst)-, calretinin (CR)-, vasoactive intestinal peptide-, and neuropeptide Y (NPY)-positive interneurons; exhibit decreased inhibitory synaptic activity in some brain regions; and subsequently develop epilepsy (31). Our results show that secondary to the in vivo interneuron loss is a homeostatic reduction in mEPSC frequency, decreased AMPA/NMDA ratio, and decreased intrinsic excitability in CA1 pyramidal neurons (that do not express *Dlx1*). Transplantation of GABA progenitor cells from the medial ganglionic eminence (MGE) (34) causes a reversal of the homeostatic changes in excitatory synaptic activity and Rin. Additionally, we describe unique changes in $Dlx1^{-/-}$ circuit function that homeostatic compensation does not correct: enhanced long-term potentiation (LTP) and altered gamma frequency oscillations (GFOs). The severity of these phenotypes is reduced by interneuron transplantation. These studies demonstrate the responsiveness of excitatory circuitry to changes in inhibition, using homeostatic plasticity as a mechanism for maintaining excitatory/inhibitory balance.

Significance

We describe homeostatic plasticity of both excitatory synaptic transmission and intrinsic properties of CA1 pyramidal neurons in distal-less homeobox 1 ($Dlx1^{-/-}$) mice, a genetic model of postdevelopment interneuron cell death. Loss of synaptic inhibition and compensation by excitation led to enhanced potential for long-term potentiation (LTP) and altered neural oscillations. This shows that homeostatic compensation may rebalance inhibition and excitation but cannot fully normalize neural function. Transplantation of interneuron progenitor cells restored inhibitory synaptic transmission to WT levels and induced a reversal of homeostatic changes to excitation and excitability. LTP and gamma oscillations were also normalized after integration of transplanted interneurons. These data indicate that homeostatic plasticity functions in vivo to balance activity based on inhibitory tone.

Results

MGE Progenitor Cells Integrate into Neural Circuitry. Following postnatal transplantation into neocortex, MGE progenitor cells migrate and mature into functional GABAergic inhibitory interneurons (34). Transplanted interneurons form direct inhibitory synaptic connections and increase inhibitory tone onto native pyramidal neurons, as measured with single- or dual-patch recordings and with EM (34–36). Once a ceiling of enhanced inhibitory tone is reached, transplantation of greater numbers of interneuron progenitors no longer increases synaptic inhibition (37). We transplanted dissociated MGE cells from β-actin–GFP mouse embryonic day (E) 13 into the dorsal hippocampus of WT postnatal day (P) 2 mouse pups. At P35 (or 32 d after transplantation), immunohistochemistry was performed using neuron- and interneuron-specific markers. GFP$^+$ cells migrated widely and could be seen throughout the dorsal hippocampus (Fig. 1A and Fig. S1). Many GFP$^+$ cells colabeled for the neuron-specific marker NeuN or for biomarkers of MGE-derived interneurons, Sst and parvalbumin (PV), whereas only a small fraction colabeled for NPY, CR, or GFAP (Fig. 1B and Table S1). Recordings from

GFP$^+$ cells in hippocampal slices from transplanted mice at P35 revealed AP firing patterns indicative of mature interneurons (Fig. 1C) and spontaneous excitatory postsynaptic currents (sEPSCs) (Fig. 1C). These findings are consistent with an MGE lineage and confirm the functional integration of MGE-derived interneurons into the host hippocampal circuitry.

Inhibitory Synaptic Activity in *Dlx1*$^{-/-}$ Hippocampus Is Normalized by MGE Transplantation. *Dlx1* is widely expressed in MGE- and lateral ganglionic eminence-derived interneuron progenitor cells during embryonic development (38). Sst$^+$, CR$^+$, and NPY$^+$ interneurons maintain such expression into adulthood (31, 39). In *Dlx1*$^{-/-}$ mice, a subset of these *Dlx1*$^+$ interneurons undergo apoptotic cell death between P21 and P30, resulting in decreased synaptic inhibition onto CA3 hippocampal and layer 2/3 cortical pyramidal neurons (31). Here, we measured mIPSCs in CA1 pyramidal neurons before and after this period of interneuron apoptosis. At P21, mIPSC amplitude and frequency in *Dlx1*$^{-/-}$ mice were comparable to WT (Fig. 2 A–C and Table S2). However, at P35, mIPSC frequency was significantly reduced in *Dlx1*$^{-/-}$ mice compared with WT. This deficit was reduced in *Dlx1*$^{-/-}$ mice receiving MGE transplantation (Tr-*Dlx1*$^{-/-}$) at P2 (Fig. 2 D and E; WT = 12.57 ± 0.66 Hz, $n = 27$; *Dlx1*$^{-/-}$ = 9.87 ± 0.71, $n = 27$; Tr-*Dlx1*$^{-/-}$ = 12.40 ± 0.88, $n = 12$; WT vs. *Dlx1*$^{-/-}$, $P = 0.018$; *Dlx1*$^{-/-}$ vs. Tr-*Dlx1*$^{-/-}$, $P = 0.079$; one-way ANOVA, Holm–Sidak post hoc test); mIPSC amplitude (Fig. 2F and Table S2) was unchanged in *Dlx1*$^{-/-}$ mice compared with WT. As in previous studies (34–36), transplantation of "dead" MGE cells (exposed to several freeze/thaw cycles) into *Dlx1*$^{-/-}$ mice induced no increase in mIPSC frequency compared with nontransplanted *Dlx1*$^{-/-}$ mice (Fig. S2). In this experiment and some to follow, Tr-*Dlx1*$^{-/-}$ groups exhibited higher variability compared with WT and *Dlx1*$^{-/-}$ groups. Factors increasing variability in these data could include the following: numbers of cells transplanted, location of transplant, or location of transplanted cells relative to recorded pyramidal cells. However, to maintain objectivity, we did not exclude data on the basis of the perceived effectiveness of the transplant. Although P2 MGE transplantation increased the number of Sst$^+$ interneurons in the hippocampus, it did not lessen the cell death of native Sst$^+$ interneurons in *Dlx1*$^{-/-}$ mice (Fig. S1), further indicating that recovery of synaptic inhibition following transplantation was due to integration of transplanted interneurons.

Homeostatic Reductions in Excitatory Drive onto CA1 Pyramidal Neurons in *Dlx1*$^{-/-}$ Mice. Although homeostatic synaptic plasticity has been studied extensively in vitro (15, 40, 41), little is known about the role it plays in neurological abnormalities such as interneuronopathy. As with synaptic inhibition, before interneuron loss, mEPSC amplitude and frequency were normal in P21 *Dlx1*$^{-/-}$ mice (Fig. 3 A–C and Table S3). However, mEPSC frequency was significantly reduced at P35 in *Dlx1*$^{-/-}$ mice compared with both WT and Tr-*Dlx1*$^{-/-}$ mice (Fig. 3 D and E; WT = 0.409 ± 0.021, $n = 15$; *Dlx1*$^{-/-}$ = 0.286 ± 0.032, $n = 11$; Tr-*Dlx1*$^{-/-}$ = 0.424 ± 0.025, $n = 36$; WT vs. *Dlx1*$^{-/-}$, $P = 0.010$; *Dlx1*$^{-/-}$ vs. Tr-*Dlx1*$^{-/-}$, $P = 0.041$; one-way ANOVA, Holm–Sidak post hoc test). As with mIPSCs, mEPSC frequency was not changed in *Dlx1*$^{-/-}$ mice after transplantation of dead MGE cells (Fig. S2). The mEPSC amplitude (Fig. 3F) and kinetics (Table S3) were unchanged across groups. Note that *Dlx1* is not expressed in the pre- or postsynaptic excitatory neurons recorded from these hippocampal regions and that pyramidal neuron morphology and numbers are normal in both of these hippocampal regions (38, 42). These data suggest that decreased excitatory neurotransmission is not a primary phenotype of the *Dlx1*$^{-/-}$ mouse but rather evolves from an in vivo homeostatic decrease in the power of excitatory synaptic input following decreases in the power of inhibition in the circuit or arrested development of excitatory transmission at the time of inhibitory cell loss. Other
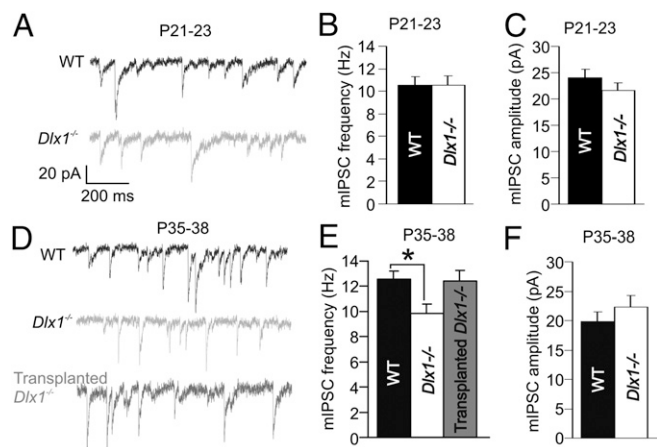

Fig. 1. Transplanted MGE precursors integrate into the circuitry of the hippocampus. (A, Left) Schematic illustrates MGE transplantation: Progenitor cells are collected from E13 embryos for transplantation into P2 pups; experiments were performed at P35. IHC, immunohistochemistry. (A, Right) Representative coronal section of the dorsal hippocampus made at P35 (33 days after transplantation) shows transplanted β-actin–GFP$^+$ interneurons filling the hippocampus. (Scale bar: 200 μm). (B, Left) Immunohistochemistry labeling for interneuron markers (Upper) and colabeling for transplanted interneurons (Lower) shows mature GFP$^+$ neurons of MGE subtypes. (Scale bar: 100 μm.) (B, Right) Quantification of colabeling for various biomarkers ($n = 5$ for each marker). PV, parvalbumin. (C) Example of electrophysiological recordings from transplanted GFP$^+$ cells made at P35. Most GFP$^+$ cells exhibited fast-spiking (Left) or regular-spiking nonpyramidal (Center) phenotypes. (Right) All GFP$^+$ neurons recorded exhibited sEPSCs.

Fig. 2. Inhibitory synaptic transmission in CA1 pyramidal cells decreases after interneuronopathy in $Dlx1^{-/-}$ mice. (A–C) mIPSCs are normal in amplitude ($P = 0.28$, paired t test) and frequency ($P = 0.98$, paired t test) in P21 $Dlx1^{-/-}$ mice. (Scale bars in A apply to all traces in this figure.) (D and E) At P35, after interneuron cell death, mIPSC frequency is significantly reduced in $Dlx1^{-/-}$ mice compared with WT littermates. (F) mIPSC amplitude at P35 was unchanged across groups (*$P > 0.05$, one-way ANOVA).

experiments were performed to study the correlation between inhibition and excitation in single pyramidal cells. Spontaneous inhibitory postsynaptic current (sIPSC) and sEPSC frequencies exhibited patterns similar to miniature synaptic events in that $Dlx1^{-/-}$ neurons showed significant decreases, whereas neurons from Tr-$Dlx1^{-/-}$ mice showed WT levels of activity; however, when sEPSC frequency was plotted as a function of sIPSC frequency for single cells for any experimental group or across all groups, no significant correlation was found (Fig. S3). The lack of statistically significant correlation between sIPSCs and sEPSCs could be due to factors such as variability of the two measures, differential activity levels among cell types in acute slices, and the indirect nature of in vitro measures relative to in vivo activity levels.

Reductions to mEPSC frequency can arise from changes to either the pre- or postsynaptic machinery. To examine these possibilities, we recorded the paired pulse ratio (PPR; an indicator of the presynaptic release probability) and AMPA/NMDA ratio of EPSCs in CA1 pyramidal neurons. The PPR was unchanged in $Dlx1^{-/-}$ mice relative to control or Tr-$Dlx1^{-/-}$ mice (Fig. 3G). However, the AMPA/NMDA ratio was significantly reduced in $Dlx1^{-/-}$ mice and normalized by MGE transplantation (Fig. 3H; WT = 4.05 ± 0.37, $n = 13$; $Dlx1^{-/-}$ = 2.75 ± 0.23, $n = 18$; Tr-$Dlx1^{-/-}$ = 3.77 ± 0.36, $n = 16$; WT vs. $Dlx1^{-/-}$, $P = 0.021$; $Dlx1^{-/-}$ vs. Tr-$Dlx1^{-/-}$, $P = 0.048$; one-way ANOVA, Holm–Sidak post hoc test). To examine changes to synaptic excitation further, input/output (I/O) functions of field excitatory postsynaptic potentials (fEPSPs) were recorded in CA1 of WT and $Dlx1^{-/-}$ slices. Although significant reductions in fEPSP slope were seen at each level of the I/O function in $Dlx1^{-/-}$ slices, isolated NMDA fEPSPs were unchanged between the genotypes (Fig. S4). These findings suggest that reduced synaptic inhibition leads to postsynaptic homeostatic excitatory plasticity, resulting in a greater number of silent glutamatergic synapses in $Dlx1^{-/-}$ pyramidal neurons.
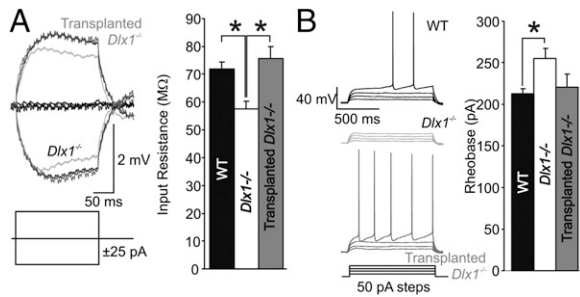
Intrinsic Excitability of CA1 Pyramidal Neurons Is Reduced in $Dlx1^{-/-}$ Mice. AP threshold and dynamics are also subject to activity-induced plasticity, via changes in the number or subcellular distribution of K$^+$ and Na$^+$ channels (24–29). We examined the excitability of CA1 pyramidal neurons in mice before and after interneuron loss. In current-clamp recordings, Rin was significantly reduced in P35 $Dlx1^{-/-}$ mice compared with WT, and this

phenotype was rescued to WT levels in Tr-$Dlx1^{-/-}$ mice (Fig. 4A; WT = 71.76 ± 2.73 MΩ, $n = 20$; $Dlx1^{-/-}$ = 57.54 ± 2.82, n = 21; Tr-$Dlx1^{-/-}$ = 75.69 ± 4.20, $n = 17$; WT vs. $Dlx1^{-/-}$, $P < 0.001$; $Dlx1^{-/-}$ vs. Tr-$Dlx1^{-/-}$, $P = 0.004$; one-way ANOVA, Holm–Sidak post hoc test). Because Rin changes can directly alter excitability, we also measured the rheobase (amplitude of a long current step required to evoke spikes). The rheobase was significantly higher in P35 $Dlx1^{-/-}$ neurons compared with WT, but it was not fully recovered following MGE transplantation (Fig. 4B; WT = 212.5 ± 5.88 MΩ, $n = 20$; $Dlx1^{-/-}$ = 254.76 ± 12.39, $n = 21$; Tr-$Dlx1^{-/-}$ = 220.59 ± 15.93, $n = 17$; WT vs. $Dlx1^{-/-}$, $P < 0.033$; one-way ANOVA on ranks, Dunn's post hoc test). AP properties in P35 $Dlx1^{-/-}$ neurons revealed a significant narrowing of AP half-width and the number of spikes evoked by a 1-s, 500-pA current step in $Dlx1^{-/-}$ mice compared with WT but no changes to AP voltage threshold or AP amplitude (Table S4). As with the homeostatic synaptic compensation described earlier, the changes to neuronal intrinsic properties were largely reversed in Tr-$Dlx1^{-/-}$ mice. Thus, in this model of in vivo changes to synaptic inhibition, homeostatic plasticity of intrinsic properties affects passive conductances and/or voltage-activated K$^+$ channels but not Na$^+$ channels.

Long-Term Synaptic Plasticity Is Altered in $Dlx1^{-/-}$ Mice and Normalized by Rescue of Inhibition. Schaffer collateral LTP results from synapse-specific insertion of AMPA receptors into synapses activated synchronous with postsynaptic activity (43). We measured LTP in acute
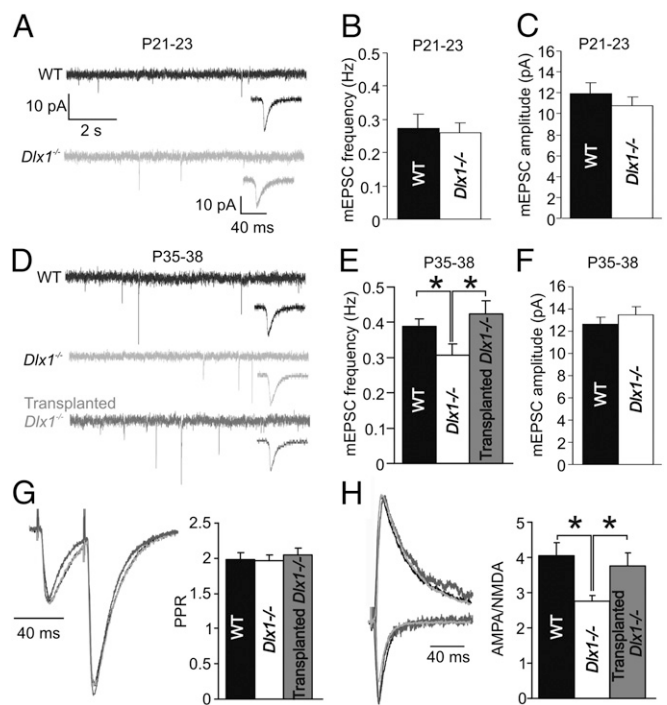
Fig. 3. Homeostatic changes to excitatory synaptic transmission in CA1 pyramidal cells of $Dlx1^{-/-}$ mice. (A–C) mEPSCs were normal in amplitude ($P = 0.43$, paired t test) and frequency ($P = 0.77$, paired t test) in $Dlx1^{-/-}$ mice at P21. (Insets) Averaged mEPSCs on an expanded time scale. (Large scale bars in A apply to all extended traces, whereas small scale bars apply to all Inset traces.) (D and E) At P35, mEPSC frequency was significantly reduced in $Dlx1^{-/-}$ mice compared with WT; however, mEPSC frequency was normalized by MGE transplantation (WT vs. $Dlx1^{-/-}$, *$P = 0.01$; $Dlx1^{-/-}$ vs. Tr-$Dlx1^{-/-}$, *$P = 0.048$). (F) mEPSC amplitude was unchanged across groups ($P = 0.40$, paired t test). (G) PPR of evoked EPSCs (40-ms interstimulus interval) was unchanged across groups ($P = 0.86$; one-way ANOVA). (H) AMPA/NMDA of evoked EPSCs was significantly reduced in $Dlx1^{-/-}$ mice compared with both WT and Tr-$Dlx1^{-/-}$ mice (WT vs. $Dlx1^{-/-}$, *$P = 0.021$; $Dlx1^{-/-}$ vs. Tr-$Dlx1^{-/-}$, *$P = 0.048$).

Fig. 4. Homeostatic plasticity of intrinsic properties reduces CA1 pyramidal cell excitability after interneuronopathy. (A) Rin, induced by 25-pA steps in current-clamp recordings, is significantly reduced in P35 $Dlx1^{-/-}$ mice compared with WT and is rescued by MGE transplantation (WT vs. $Dlx1^{-/-}$, *P < 0.001; $Dlx1^{-/-}$ vs. Tr-$Dlx1^{-/-}$, *P = 0.004). (B) Rheobase is significantly increased at P35 in $Dlx1^{-/-}$ mice compared with WT (WT vs. $Dlx1^{-/-}$, *P < 0.033).

hippocampal slices from P35 WT, $Dlx1^{-/-}$, and Tr-$Dlx1^{-/-}$ mice in response to high-frequency stimulation. One hour after LTP induction, the fEPSP slope showed significant potentiation for all groups (Fig. 5). LTP was significantly enhanced in $Dlx1^{-/-}$ mice compared with WT (WT = 140.0 ± 7.74%, n = 14; $Dlx1^{-/-}$ = 173.1 ± 9.22, n = 13; Tr-$Dlx1^{-/-}$ = 150.5 ± 8.41, n = 13; WT vs. $Dlx1^{-/-}$, P = 0.039; one-way ANOVA on ranks, Dunn's post hoc test). A larger population of silent synapses in pyramidal neurons of $Dlx1^{-/-}$ mice, as suggested above, could provide a potential mechanism for enhanced LTP.

Abnormal Gamma Oscillations in $Dlx1^{-/-}$ Mice Are Rescued by MGE Transplantation. GFOs are related to the firing of local populations of neurons entrained by an electrical syncytium of parvalbumin-positive interneurons (44). GFOs are transient, often correlated with cognitive operations, and altered in neuropsychiatric diseases such as schizophrenia and autism (both of which may be interneuronopathy-related). Using EEG head mounts designed for seizure monitoring, we measured cortical local field potentials (LFPs) in awake, freely behaving P35-40 WT, $Dlx1^{-/-}$, and Tr-$Dlx1^{-/-}$ mice and quantified power across specific frequency bands of the power spectra (Fig. 6A and Table S5). Frequency bands of interest (theta = 5–10 Hz, gamma = 25–90 Hz, high gamma = 90–130 Hz) were defined before analysis based on previous reports (45). Averaged across a 5-min epoch, mean power at theta and gamma was not significantly different across groups (Fig. 6 A and C and Fig. S5). However, because GFOs are transient events, we monitored power in the gamma frequency band over time across a 5-min epoch (Fig. 6B), revealing large peaks in gamma power, particularly in $Dlx1^{-/-}$ mice. Peak gamma power was significantly increased in $Dlx1^{-/-}$ mice compared with WT and Tr-$Dlx1^{-/-}$ mice (Fig. 6D; WT = 7.24 * 10^{-3} ± 0.66 * 10^{-3} μV^2/Hz, n = 5; $Dlx1^{-/-}$ = 12.0 * 10^{-3} ± 1.48 * 10^{-3} μV^2/Hz, n = 5; Tr-$Dlx1^{-/-}$ = 6.90 * 10^{-3} ± 0.72 * 10^{-3} μV^2/Hz, n = 5; WT vs. $Dlx1^{-/-}$, P = 0.012; $Dlx1^{-/-}$ vs. Tr-$Dlx1^{-/-}$, P = 0.013; one-way ANOVA, Holm–Sidak post hoc test). We propose two hypotheses by which hippocampal transplantation could lead to differences in cortical oscillations. Transplanted interneurons often migrate up the needle tract out of the hippocampus and into the cortex and integrate there, thus providing direct, local changes to inhibition. Alternately, transplantation could normalize hippocampal activity patterns, thus providing WT-like input patterns to the cortical microcircuit and an indirect mechanism by which cortical oscillations are altered. Although changes in cortical oscillations are indirect measures of neural activity, such in vivo differences in EEG recordings are correlated with human diseases, such as epilepsy, autism, and schizophrenia, and may serve as an early biomarker for the onset

of neurological disease. Cobos et al. (31) described changes to theta rhythms in $Dlx1^{-/-}$ mice. We found no significant differences in mean power or peak power across groups (Fig. S5 and Table S5), but power at certain frequencies within the theta band and between theta and gamma appear shifted across groups (Fig. 6A) and such changes could be an interesting avenue of future investigation. Changes to cortical oscillations in $Dlx1^{-/-}$ mice are an indication of an abnormality in circuit function in $Dlx1^{-/-}$ mice not corrected for by homeostatic compensation but normalized by interneuron transplantation.

Discussion

We demonstrate that homeostatic synaptic and intrinsic plasticity occurs in vivo in the adult brain in response to changes in interneuron number and synaptic inhibition. The homeostatic changes described did not normalize all circuit function after interneuronopathy, as illustrated by abnormal LTP and GFOs in $Dlx1$ mutant mice. However, many of the phenotypes induced by interneuronopathy were rescued to control levels by neonatal interneuron transplantation, indicating that homeostatic plasticity dynamically changes excitability bidirectionally, as activity levels change following loss or addition (via transplantation) of interneurons.

Homeostatic plasticity describes a diverse array of synaptic and intrinsic mechanisms by which neurons maintain firing levels within a specific range in the face of changing conditions. These changes are cell-autonomous and can be induced by changes to a neuron's firing rate alone (without regard to actual levels of synaptic input), and they are triggered via molecular sensors of activity-induced calcium influx (18). Although the classic studies of homeostatic synaptic plasticity describe mainly increases in the amplitude of EPSCs (15), recent studies and our own data describe changes to event frequency related to both probability of presynaptic release and synapse number (16). Notably, although the phenomenon was originally described in neuronal culture systems, recent reports have described synaptic scaling in vivo following sensory deprivation (25, 46) and cortical injury (47). The ability of neurons to self-regulate output levels across a range of input conditions begs the question as to whether homeostatic plasticity is a mechanism of neuroprotection during pathological states of hyperexcitability. Interestingly, some data suggest that although homeostatic plasticity may be protective at the level of individual cells, such changes are ineffective at maintaining normality of, and are potentially disruptive to, circuit function under pathological conditions (48). Increasing the strength of remaining excitatory synaptic inputs after partial deafferentation increases the excitatory power of a reduced number of presynaptic partners. In the undercut model of cortical trauma,
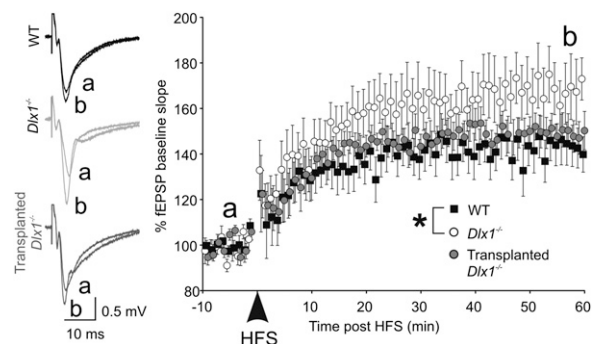
Fig. 5. $Dlx1^{-/-}$ mice exhibit enhanced LTP after interneuronopathy. The fEPSPs were stimulated at 0.05 Hz for 10 min before (a) and 1 h following (b) high-frequency stimulation (HFS; 4 × 1-s, 100-Hz bursts; 20-s interburst interval) in P35 mice. One hour after HFS (b), the LTP of the fEPSP slope was significantly increased in $Dlx1^{-/-}$ mice compared with WT.

NEUROSCIENCE
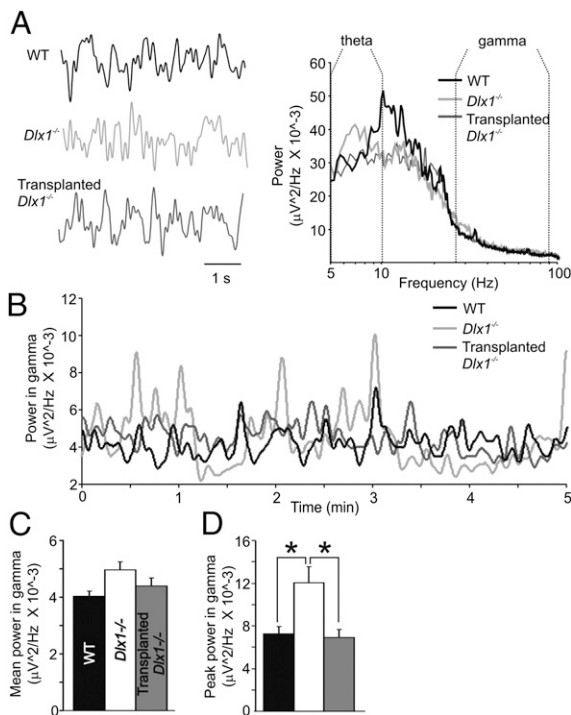
Fig. 6. Gamma oscillations are abnormally increased in *Dlx1*$^{-/-}$ mice after interneuronopathy and are rescued by MGE transplantation. (*A, Left*) LFPs recorded with subdural electrodes in P35 WT, *Dlx1*$^{-/-}$, and Tr-*Dlx1*$^{-/-}$ mice. (*A, Right*) Power spectra of these signals averaged over a 5-min epoch. (*B*) Power in the gamma frequency band (25–90 Hz) changes as a function of time. (*C*) Mean power across the 5-min epoch displayed in *A* exhibits a nonsignificant trend (*P* = 0.079; one-way ANOVA). (*D*) Peak power in the gamma frequency band is significantly increased in *Dlx1*$^{-/-}$ mice compared with WT and is rescued by MGE transplantation (WT vs. *Dlx1*$^{-/-}$, **P* = 0.012; *Dlx1*$^{-/-}$ vs. Tr-*Dlx1*$^{-/-}$, **P* = 0.013).

homeostatic changes result in reduced convergence (i.e., fewer presynaptic partners) and increased input strength onto a neuron (47). In a system requiring presynaptic synchrony to drive activity, increasing the excitatory power of each of a decreased number of presynaptic partners could raise the probability of feed-forward excitation, which could contribute to epileptogenesis. Here, we show homeostatic plasticity in *Dlx1*$^{-/-}$ mice, which suffer from adult-onset interneuronopathy followed months later by the development of epilepsy. Similar to the examples above, homeostatic silencing of synapses reduces convergence onto CA1 pyramidal neurons, thus granting control of neuronal output to a smaller than normal number of inputs. Thus, the question of neuroprotection by homeostatic plasticity remains open: The homeostatic compensations documented here reduce excitotoxic damage to these neurons, but decreased convergence and a reduced number of presynaptic partners to synchronize offer a mechanism by which seizure probability could actually increase.

Our data show enhanced LTP in *Dlx1*$^{-/-}$ mice after interneuronopathy and homeostatic compensation have taken place. Although LTP can be induced via a variety of mechanisms in different cell types, a major mechanism of LTP at Schaffer collateral synapses is insertion of AMPA receptors into the postsynaptic membrane (49). Our data suggest that homeostatic compensation results in a larger than usual number of silent synapses in *Dlx1*$^{-/-}$ CA1 neurons, the unsilencing of which provides a candidate mechanism for greater potential LTP. It remains to be seen whether maintaining this population of silent synapses is adaptive or maladaptive for the circuit; silent synapses could allow for a return to normal levels of convergence upon recovery of

inhibition. Another possibility is that greater synaptic potentiation could contribute to future hyperexcitability. Unsilencing and potentiation across a large number of synapses induced by a period of high circuit activity could further contribute to the pathological hyperexcitability and epileptic phenotype exhibited by these mice at older ages (31). Alterations in LTP potential following interneuron loss thus provide a cellular mechanism by which learning and cognitive disturbances could arise in other neurological diseases in which interneuronopathy is present.

Aberrant GFOs reflect altered levels of synchronous neural activity (50) and have been reported in interneuronopathy-related neurological diseases (51–54). That changes to GFOs might be measurable in disorders associated with interneuronopathy is not a coincidence. The synchronous neural activity required to produce GFOs is linked to rhythmic firing by the electrically coupled network of PV$^+$ interneurons at gamma frequencies, which, in turn, phase-locks feed-forward excitatory activity through the microcircuit (55, 56). Additionally, the perisomatic location of their strong inhibitory synapses onto pyramidal cells provides a mechanism by which PV interneurons can entrain activity among the excitatory cells of the circuit (57). The precise mechanism underlying transient increases in GFO power recorded in *Dlx1*$^{-/-}$ mice is unclear. PV$^+$ interneurons do not undergo apoptosis during interneuronopathy in this model. This raises the proportion of PV$^+$ interneurons relative to the entire population of GABAergic interneurons, increasing the relative power of inhibition by this cell type. PV$^+$ interneurons were also found to receive enhanced excitatory drive in adult *Dlx1*$^{-/-}$ mice (42). As such, one hypothesis for GFO changes in *Dlx1*$^{-/-}$ mice is a greater level of activity in the PV/interneuron network relative to other sources of inhibition.

Our data illustrate that cell-autonomous homeostatic plasticity occurs bidirectionally in excitatory neurons in vivo after interneuron cell death and replacement via progenitor transplantation. We identified neural circuit abnormalities, namely LTP and GFO changes, that were not corrected by homeostatic plasticity but were partly rescued by interneuron transplantation. These findings have important implications for controlling excitatory/inhibitory balance and homeostatic plasticity under both normal and pathological conditions, via manipulation of interneurons.

Materials and Methods

In Vitro Slice Physiology. The University of California, San Francisco Institutional Animal Care and Use Committee approved all protocols and procedures described. Acute slice electrophysiological recordings were performed as in previous reports (38). Briefly, 300-μm coronal sections of the whole brain were made in ice-cold artificial cerebrospinal fluid (ACSF), incubated at 35 °C, and then held at room temperature. Recordings of CA1 neurons were made at 35 °C using 3–5 ΩM borosilicate electrodes. Pipette solution for EPSC recording was cesium methanesulfonate-based, whereas IPSC recordings were made with a cesium chloride solution, and current-clamp recordings were made with potassium gluconate solution (38). The mIPSCs were pharmacologically isolated by the addition of kynurenic acid (3 mM) and TTX (0.1 μM) to the ACSF, and EPSCs were isolated with TTX and gabazine (100 μM). Recordings in which sIPSCs and sEPSCs were made from single neurons were accomplished using a cesium gluconate solution. The sIPSCs were recorded at a holding potential of 0 mV, and the sEPSCs were recorded at a holding potential of −70 mV.

Immunohistochemistry. Brains fixed in paraformaldehyde [4% (wt/vol) in PBS] brains were cut in 50-μm coronal sections. The following primary antibodies were used (species; source): calbindin, CR (rabbit; Chemicon), GAD67 (mouse monoclonal; Millipore), GFP (chicken; Aves), NPY (rabbit; Immunostar), parvalbumin (mouse monoclonal; Sigma), and Sst (rat; Chemicon). Secondary antibodies used were anti-chicken Alexa Fluor 488, anti-mouse Alexa Fluor 594, and anti-rabbit Alexa Fluor 594 (all from Molecular Probes).

MGE Progenitor Transplantation. Male transgenic mice homozygous for beta-actin promoter-driven GFP were bred with CD-1 female mice. MGEs were isolated from E13 embryos, and dissociated MGE cells were loaded into a glass needle and injected bilaterally into the dorsal hippocampus of anesthetized recipient pups (aged P1–P3) based on stereotaxic coordinates.

In Vivo LFP Recordings. Under anesthesia, mice were fitted with an EEG head mount (Pinnacle Technology) with four cortical surface electrodes. Rostral electrodes were located over M1, and caudal electrodes were located over V1. LFPs were recorded continuously for a period of at least 7 d using the Sirenia (Pinnacle Technology) software package. Data were analyzed using custom software written in MATLAB R2011 (MathWorks).

1. Davis GW, Bezprozvanny I (2001) Maintaining the stability of neural function: A homeostatic hypothesis. *Annu Rev Physiol* 63:847–869.
2. Turrigiano G (2011) Too many cooks? Intrinsic and synaptic homeostatic mechanisms in cortical circuit refinement. *Annu Rev Neurosci* 34:89–103.
3. Buckmaster PS, Jongen-Rêlo AL (1999) Highly specific neuron loss preserves lateral inhibitory circuits in the dentate gyrus of kainate-induced epileptic rats. *J Neurosci* 19(21):9519–9529.
4. Busche MA, et al. (2008) Clusters of hyperactive neurons near amyloid plaques in a mouse model of Alzheimer's disease. *Science* 321(5896):1686–1689.
5. Cossart R, et al. (2001) Dendritic but not somatic GABAergic inhibition is decreased in experimental epilepsy. *Nat Neurosci* 4(1):52–62.
6. Dinocourt C, Petanjek Z, Freund TF, Ben-Ari Y, Esclapez M (2003) Loss of interneurons innervating pyramidal cell dendrites and axon initial segments in the CA1 region of the hippocampus following pilocarpine-induced seizures. *J Comp Neurol* 459(4):407–425.
7. Han S, et al. (2012) Autistic-like behaviour in Scn1a+/- mice and rescue by enhanced GABA-mediated neurotransmission. *Nature* 489(7416):385–390.
8. de Lanerolle NC, Kim JH, Robbins RJ, Spencer DD (1989) Hippocampal interneuron loss and plasticity in human temporal lobe epilepsy. *Brain Res* 495(2):387–395.
9. Li G, et al. (2009) GABAergic interneuron dysfunction impairs hippocampal neurogenesis in adult apolipoprotein E4 knockin mice. *Cell Stem Cell* 5(6):634–645.
10. Palop JJ, et al. (2007) Aberrant excitatory neuronal activity and compensatory remodeling of inhibitory hippocampal circuits in mouse models of Alzheimer's disease. *Neuron* 55(5):697–711.
11. Peñagarikano O, et al. (2011) Absence of CNTNAP2 leads to epilepsy, neuronal migration abnormalities, and core autism-related deficits. *Cell* 147(1):235–246.
12. Rubenstein JLR, Merzenich MM (2003) Model of autism: Increased ratio of excitation/inhibition in key neural systems. *Genes Brain Behav* 2(5):255–267.
13. Burrone J, O'Byrne M, Murthy VN (2002) Multiple forms of synaptic plasticity triggered by selective suppression of activity in individual neurons. *Nature* 420(6914):414–418.
14. Ibata K, Sun Q, Turrigiano GG (2008) Rapid synaptic scaling induced by changes in postsynaptic firing. *Neuron* 57(6):819–826.
15. Turrigiano GG, Leslie KR, Desai NS, Rutherford LC, Nelson SB (1998) Activity-dependent scaling of quantal amplitude in neocortical neurons. *Nature* 391(6670):892–896.
16. Wierenga CJ, Walsh MF, Turrigiano GG (2006) Temporal regulation of the expression locus of homeostatic plasticity. *J Neurophysiol* 96(4):2127–2133.
17. Gainey MA, Hurvitz-Wolff JR, Lambo ME, Turrigiano GG (2009) Synaptic scaling requires the GluR2 subunit of the AMPA receptor. *J Neurosci* 29(20):6479–6489.
18. Goold CP, Nicoll RA (2010) Single-cell optogenetic excitation drives homeostatic synaptic depression. *Neuron* 68(3):512–528.
19. Kilman V, van Rossum MCW, Turrigiano GG (2002) Activity deprivation reduces miniature IPSC amplitude by decreasing the number of postsynaptic GABA(A) receptors clustered at neocortical synapses. *J Neurosci* 22(4):1328–1337.
20. Maffei A, Nataraj K, Nelson SB, Turrigiano GG (2006) Potentiation of cortical inhibition by visual deprivation. *Nature* 443(7107):81–84.
21. Hartman KN, Pal SK, Burrone J, Murthy VN (2006) Activity-dependent regulation of inhibitory synaptic transmission in hippocampal neurons. *Nat Neurosci* 9(5):642–649.
22. Rosato-Siri M, Grandolfo M, Ballerini L (2002) Activity-dependent modulation of GABAergic synapses in developing rat spinal networks in vitro. *Eur J Neurosci* 16(11):2123–2135.
23. Lau CG, Murthy VN (2012) Activity-dependent regulation of inhibition via GAD67. *J Neurosci* 32(25):8521–8531.
24. Aptowicz CO, Kunkler PE, Kraig RP (2004) Homeostatic plasticity in hippocampal slice cultures involves changes in voltage-gated Na+ channel expression. *Brain Res* 998(2):155–163.
25. Breton J-D, Stuart GJ (2009) Loss of sensory input increases the intrinsic excitability of layer 5 pyramidal neurons in rat barrel cortex. *J Physiol* 587(Pt 21):5107–5119.
26. Desai NS, Rutherford LC, Turrigiano GG (1999) Plasticity in the intrinsic excitability of cortical pyramidal neurons. *Nat Neurosci* 2(6):515–520.
27. Nelson AB, Gittis AH, du Lac S (2005) Decreases in CaMKII activity trigger persistent potentiation of intrinsic excitability in spontaneously firing vestibular nucleus neurons. *Neuron* 46(4):623–631.
28. Grubb MS, Burrone J (2010) Activity-dependent relocation of the axon initial segment fine-tunes neuronal excitability. *Nature* 465(7301):1070–1074.
29. Kuba H, Oichi Y, Ohmori H (2010) Presynaptic activity regulates Na(+) channel distribution at the axon initial segment. *Nature* 465(7301):1075–1078.
30. Echegoyen J, Neu A, Graber KD, Soltesz I (2007) Homeostatic plasticity studied using in vivo hippocampal activity-blockade: Synaptic scaling, intrinsic plasticity and age-dependence. *PLoS ONE* 2(8):e700.
31. Cobos I, et al. (2005) Mice lacking Dlx1 show subtype-specific loss of interneurons, reduced inhibition and epilepsy. *Nat Neurosci* 8(8):1059–1068.
32. Seybold BA, et al. (2012) Chronic reduction in inhibition reduces receptive field size in mouse auditory cortex. *Proc Natl Acad Sci USA* 109(34):13829–13834.
33. Alvarez-Dolado M, et al. (2006) Cortical inhibition modified by embryonic neural precursors grafted into the postnatal brain. *J Neurosci* 26(28):7380–7389.
34. Mao R, et al. (2012) Influence of a subtype of inhibitory interneuron on stimulus-specific responses in visual cortex. *Cereb Cortex* 22(3):493–508.
35. Southwell DG, Froemke RC, Alvarez-Buylla A, Stryker MP, Gandhi SP (2010) Cortical plasticity induced by inhibitory neuron transplantation. *Science* 327(5969):1145–1148.
36. Baraban SC, et al. (2009) Reduction of seizures by transplantation of cortical GABAergic interneuron precursors into Kv1.1 mutant mice. *Proc Natl Acad Sci USA* 106(36):15472–15477.
37. Southwell DG, et al. (2012) Intrinsically determined cell death of developing cortical interneurons. *Nature* 491(7422):109–113.
38. Anderson SA, Eisenstat DD, Shi L, Rubenstein JLR (1997) Interneuron migration from basal forebrain to neocortex: Dependence on Dlx genes. *Science* 278(5337):474–476.
39. Cobos I, Long JE, Thwin MT, Rubenstein JL (2006) Cellular patterns of transcription factor expression in developing cortical interneurons. *Cereb Cortex* 16(Suppl 1):i82–i88.
40. Kim J, Tsien RW (2008) Synapse-specific adaptations to inactivity in hippocampal circuits achieve homeostatic gain control while dampening network reverberation. *Neuron* 58(6):925–937.
41. Stellwagen D, Beattie EC, Seo JY, Malenka RC (2005) Differential regulation of AMPA receptor and GABA receptor trafficking by tumor necrosis factor-alpha. *J Neurosci* 25(12):3219–3228.
42. Jones DL, Howard MA, Stanco A, Rubenstein JLR, Baraban SC (2011) Deletion of Dlx1 results in reduced glutamatergic input to hippocampal interneurons. *J Neurophysiol* 105(5):1984–1991.
43. Kerchner GA, Nicoll RA (2008) Silent synapses and the emergence of a postsynaptic mechanism for LTP. *Nat Rev Neurosci* 9(11):813–825.
44. Sohal VS, Zhang F, Yizhar O, Deisseroth K (2009) Parvalbumin neurons and gamma rhythms enhance cortical circuit performance. *Nature* 459(7247):698–702.
45. Varga C, Golshani P, Soltesz I (2012) Frequency-invariant temporal ordering of interneuronal discharges during hippocampal oscillations in awake mice. *Proc Natl Acad Sci USA* 109(40):E2726–E2734.
46. Goel A, Lee H-K (2007) Persistence of experience-induced homeostatic synaptic plasticity through adulthood in superficial layers of mouse visual cortex. *J Neurosci* 27(25):6692–6700.
47. Avramescu S, Timofeev I (2008) Synaptic strength modulation after cortical trauma: A role in epileptogenesis. *J Neurosci* 28(27):6760–6772.
48. Howard AL, Neu A, Morgan RJ, Echegoyen JC, Soltesz I (2007) Opposing modifications in intrinsic currents and synaptic inputs in post-traumatic mossy cells: Evidence for single-cell homeostasis in a hyperexcitable network. *J Neurophysiol* 97(3):2394–2409.
49. Kessels HW, Malinow R (2009) Synaptic AMPA receptor plasticity and behavior. *Neuron* 61(3):340–350.
50. Buzsáki G, Wang X-J (2012) Mechanisms of gamma oscillations. *Annu Rev Neurosci* 35:203–225.
51. Cunningham MO, et al. (2006) Region-specific reduction in entorhinal gamma oscillations and parvalbumin-immunoreactive neurons in animal models of psychiatric illness. *J Neurosci* 26(10):2767–2776.
52. Lewis DA, Curley AA, Glausier JR, Volk DW (2012) Cortical parvalbumin interneurons and cognitive dysfunction in schizophrenia. *Trends Neurosci* 35(1):57–67.
53. Spencer KM, et al. (2003) Abnormal neural synchrony in schizophrenia. *J Neurosci* 23(19):7407–7411.
54. Orekhova EV, et al. (2007) Excess of high frequency electroencephalogram oscillations in boys with autism. *Biol Psychiatry* 62(9):1022–1029.
55. Fuchs EC, et al. (2007) Recruitment of parvalbumin-positive interneurons determines hippocampal function and associated behavior. *Neuron* 53(4):591–604.
56. Tukker JJ, Fuentealba P, Hartwich K, Somogyi P, Klausberger T (2007) Cell type-specific tuning of hippocampal interneuron firing during gamma oscillations in vivo. *J Neurosci* 27(31):8184–8189.
57. Tamás G, Buhl EH, Lörincz A, Somogyi P (2000) Proximally targeted GABAergic synapses and gap junctions synchronize cortical interneurons. *Nat Neurosci* 3(4):366–371.

NEUROSCIENCE